Geophysical Research Letters

Potential Increase in Hazard From Mediterranean Hurricane Activity With Global Warming

Juan J. González-Alemán[1] , Salvatore Pascale[2,3], Jesús Gutierrez-Fernandez[1] , Hiroyuki Murakami[3,4] , Miguel A. Gaertner[5] , and Gabriel A. Vecchi[6,7]

[1]Environmental Sciences Institute, University of Castilla-La Mancha, Toledo, Spain, [2]Atmospheric and Oceanic Sciences Program, Princeton University, Princeton, NJ, USA, [3]Geophysical Fluid Dynamics Laboratory/NOAA, Princeton, NJ, USA, [4]Cooperative Programs for the Advancement of Earth System Science, University Corporation for Atmospheric Research, Boulder, CO, USA, [5]Environmental Sciences Faculty, University of Castilla-La Mancha, Toledo, Spain, [6]Department of Geosciences, Princeton University, Princeton, NJ, USA, [7]Princeton Environmental Institute, Princeton University, Princeton, NJ, USA

Abstract Mediterranean hurricanes (Medicanes) are intense cyclones that acquire tropical characteristics, associated with extreme winds and rainfall, thus posing a serious natural hazard to populated areas along Mediterranean coasts. Understanding how Medicanes will change with global warming remains, however, a challenge, because coarse resolution and/or the lack of atmosphere-ocean coupling limit the reliability of numerical simulations. Here we investigate the Medicanes' response to global warming using a recently developed 25-km global coupled climate model, which features a realistic representation of Medicanes in present climate conditions. It is found that despite a decrease in frequency, Medicanes potentially become more hazardous in the late century, lasting longer and producing stronger winds and rainfall. These changes are associated with a more robust hurricane-like structure and are mainly confined to autumn. Thus, continued anthropogenic warming will increase the risks associated with Medicanes even in an intermediate scenario (Representative Concentration Pathway, RCP4.5), with potential natural and socioeconomic consequences.

Plain Language Summary Medicanes are damaging weather systems, which form over the Mediterranean Sea, resembling tropical cyclones. They have high impact in the public; thus, being important to understand how global warming will affect them. Due to their small scale, climate models have had limited reliability in their projections. In this work, we use an improved climate model, which realistically simulate them and has allowed us to get novel insight into how Anthropogenic Climate Change can alter their characteristics in the future. It is found that despite they are projected to decrease in their occurrence, they increase in their potential destructiveness. This is because they produce stronger winds and rainfall and they tend to last longer. Medicanes are also projected to acquire a more hurricane-like structure. These results point toward future Medicanes having potentially worrying natural and socioeconomic consequences.

1. Introduction

Medicanes arise from extratropical cyclones (ECs), which undergo a tropical transition process over the Mediterranean Sea (Emanuel, 2005a; Moscatello et al., 2008). They resemble tropical cyclones (TCs) as they develop a warm core, symmetric structure and concentric convective clouds around a central eye-like feature (Tous & Romero, 2013). Given their size of a few hundred kilometers (Gaertner et al., 2016), dynamical downscaling of global climate models (GCMs) outputs with regional climate models (RCMs) has been so far the most common method to study the impact of Anthropogenic Climate Change (ACC) on Medicanes. RCMs project a decrease in the number of Medicanes over the 21st century, accompanied by an increasing maximum wind intensity (Cavicchia et al., 2014b; Gaertner et al., 2007; Romera et al., 2017; Walsh et al., 2014). However, these results based on RCMs may have important limitations due to (1) the lack of atmospheric-ocean coupling and (2) the lack of an interactive cross-scale coupling with their GCMs (Lorenz & Jacob, 2005). These two factors can lead to: (1) misrepresent characteristics of Medicanes (Gaertner et al., 2016; Ricchi et al., 2017) and overestimate Medicanes' intensity (Akhtar et al., 2014; Schade & Emanuel, 1999), and (2) solutions over the limited domain that are dynamically inconsistent with global drivers (Køltzow et al., 2011).

Here we investigate the impact of ACC on Medicanes' activity with the High-Resolution Forecast-Oriented Low Ocean Resolution (HiFLOR; section 2) model (Murakami et al., 2015; Vecchi et al., 2014), a 25-km GCM developed at the National Oceanic and Atmospheric Administration Geophysical Fluid Dynamics Laboratory. While an atmosphere-only global model has recently been able to resolve Medicanes (Tous et al., 2016), ours is the first study in which a global coupled model at high horizontal atmospheric resolution is used to study the effect of ACC on multiple features of Medicanes. HiFLOR has proven to be a useful tool in studying the response of TCs to ACC (Bhatia et al., 2018; Murakami et al., 2017, 2018), and it features a horizontal resolution sufficiently high to resolve Medicanes' structure (supporting information Figure S1). Being a global model, HiFLOR explicitly accounts for nonlinear dynamics associated with extratropical weather systems (e.g., cutoff lows and wave breaking) and it is one of the few GCMs that is capable to capture category 4 and 5 TCs (Murakami et al., 2015). Being a coupled model, it includes wind-induced ocean mixing and representation of the oceanic mixed layer. However, due to the relatively low resolution of the ocean component of the model (see section 2.1), strong sea surface temperature (SST) gradients in small horizontal scale, which are usually present in the Mediterranean Sea (Ricchi et al., 2017), are not captured.

We perform three 50-year numerical simulations (section 2), representative of different 20-year periods: the climatological run (CLIM), representative of the climate mean state during the years 1986–2005, and the early future (EARLY) and late future (LATE) Representative Concentration Pathway (RCP4.5; van Vuuren et al., 2011) runs, representative of the multimodel projected SST and radiative forcing conditions during the periods (2016–2035) and (2081–2100), respectively. Under the RCP4.5 scenario, global temperature change is likely to be within 2 and 4 °C by the end of the 21st century, and it is compatible with measures to reduce CO_2 emissions and land use to stabilize radiative forcing at 4.5 W/m^2 by 2100 (Collins et al., 2013). In these three numerical experiments SSTs are restored, with a timescale of about 5 days, to the reference monthly SSTs climatology for each time period (section 2). This experimental setup (Bhatia et al., 2018; van der Wiel et al., 2017) prevents the development of substantial biases in SSTs arising in the freely running coupled model (Li & Xie, 2012), while still retaining the effects of air-sea interaction for timescale shorter than 5 days.

2. Methods

2.1. The HiFLOR GCM

HiFLOR (Murakami et al., 2015) is the high atmospheric resolution (grid spacing of ~25 km) version of the Forecast-Oriented Low Ocean Resolution (FLOR [Vecchi et al., 2014]) model (~50 km). FLOR was derived from the Geophysical Fluid Dynamics Laboratory Climate Model, version 2.5 (GFDL CM2.5 [Delworth et al., 2012]). CM2.5 features a ~0.5 × 0.5° atmospheric resolution with 32 vertical levels. FLOR is identical to CM2.5 but features a coarser ocean horizontal resolution (1 × 1°), which increases toward the equator. This considerably reduces running times, allowing for long integrations. Both CM2.5 and FLOR have been used in several studies on regional climate change (Bhatia et al., 2018; Delworth et al., 2016; Delworth & Zeng, 2014; Kapnick et al., 2014; Pascale et al., 2017). GFDL HiFLOR has been developed from FLOR by decreasing the horizontal grid spacing of the atmospheric/land component from 50 to 25 km, while leaving most of the subgrid-scale physical parameterizations unchanged. The ocean and ice components of HiFLOR are at a more moderate resolution (~100-km mesh), which is identical to FLOR's resolution. More information on GFDL CM2.5, FLOR, and HiFLOR is publicly available at https://www.gfdl.noaa.gov/cm2-5-and-flor/.

Relative to FLOR, HiFLOR considerably improved the simulation of the structure, global distribution, and seasonal and interannual variations of TCs (Murakami et al., 2015, 2016; Zhang et al., 2016). HiFLOR also proved to be able to simulate and predict extremely intense TCs (categories 4 and 5) and their interannual variations (Murakami et al., 2015). This represented the first time a fully coupled GCM had been able to simulate such extremely intense TCs in a multicentury simulation. This better representation of TCs and the response to climate also lead to improved skill (relative to FLOR) in predicting the frequencies of major hurricanes in the North Atlantic as well as landfalling TCs over its western regions a few months in advance (Murakami et al., 2016).

2.2. Restored-SST Simulations

To prevent the development of substantial biases in SSTs arising in the freely running coupled model, which impact the simulation as well as the response to climate variability and change of TCs (Murakami et al., 2015; Vecchi et al., 2014), while still retaining the effects of air-sea interaction for timescale shorter than 5 days, we use three restored-SST numerical experiments (50 year each). In each experiment, simulated SSTs are restored toward (1) the climatological monthly SST means during the period 1986–2005 (CLIM); (2) the sum of observed climatological monthly SST means over 1986–2005 and the multimodel projected climatological SST anomalies (by models from the Coupled Model Intercomparison Project Phase 5; see below) during the period 2016–2035 relative to 1986–2005 from the RCP4.5 scenario (EARLY); and the sum of observed climatological monthly SST means over 1986–2005 and the multimodel projected climatological SST anomalies during the period 2081–2100 from the RCP4.5 scenario (LATE). It is therefore important to note that here we run idealized simulations that are representative of each 20-year periods where interannual variability is not considered. These runs are simulations with 50 years of repeating climatology in each climate state, and thus, the 50 years in each experiment are statistically equivalent. The 20 years are the periods used to define the climatology for each state. These experiments are described in further detail in previous studies (Bhatia et al., 2018; van der Wiel et al., 2017).

In these runs, simulated SSTs are nudged toward the target SST_T while allowing high-frequency (i.e., on timescales smaller than the restoration timescale τ) SST fluctuations and air-sea interactions:

$$\frac{\partial SST(x,y,t)}{\partial t} = K(x,y,t) + \frac{1}{\tau}\left[SST(x,y,t)_T - SST(x,y,t)\right],$$

where $\partial SST/\partial t$ is the time tendency of SST in the nudged-SST experiment, K is the coupled model's tendency term for SST from the model governing equations, τ is the nudging timescale (5 days in this case), and SST_T is the target SST toward which the model is nudged (interpolated to the model time step from a monthly mean value).

2.3. Cyclonic and Medicane Detection

The detection of Medicanes is done in two steps. First, a cyclone tracking method (Picornell et al., 2001) is applied. It has been designed particularly for mesoscale cyclones and is therefore highly suited to the identification of Medicanes. The initial detection is based on the sea level pressure field, and the wind field at 700 hPa is used as an auxiliary variable for obtaining cyclone tracks. The cyclone intensity is measured by the maximum wind at 10 m every 6 hr within the cyclonic region. To focus the analysis on the most intense cyclones, only those cyclones exceeding tropical storm intensity (17.5 m/s) are considered in this work. Additionally, cyclones are required to last at least 36 hr. ECs are herein defined as those identified cyclones (in this first step) lasting at least 36 hr, of which 24 hr (not consecutively) must be over the sea, a measure of the overall cyclonic maritime activity.

The second step is to filter out those cyclones with tropical characteristics based on their thermal structure. This is done by applying the cyclone phase space (CPS) method (Hart, 2003). The CPS is a straightforward and objective method to represent the 3-D structure of cyclones and classify them. The CPS is constructed by three parameters: B, −VTL, and −VTU, derived from the geopotential field within the 900- to 600-hPa and 600- to 300-hPa layers. B measures the horizontal thermal symmetry of the cyclone within the lower layer, with positive values above 10 m indicating an asymmetric (frontal) cyclone and values below that threshold indicating a symmetric (nonfrontal) cyclone. The thermal wind parameters for the lower layer (−VTL) and the upper layer (−VTU) describe the thermal anomaly in the 3-D structure of the cyclone. Values above 0 indicate a warm core and negative values a cold core. Due to the small size of Medicanes, the calculation of the CPS parameters has been applied to a reduced radius of 150 km from the cyclone center, as opposed to the typical radius of 500 km (Hart, 2003). In this study, Medicanes are defined as the subset of cyclones, which acquire deep warm core, that is, tropical structure for at least two time steps (i.e., 12 not necessarily consecutive hours) while being over the ocean. The tropical structure is identified in the CPS as −VTL > 0 m, −VTU > 0 m, and B < 10 m. This last criterion in B is to ensure that Medicanes are nonfrontal as would be expected in a TC (Hart, 2003).

For Medicane intensity, the comparison is done with respect to the only available study (Cavicchia et al., 2014b), which analyzes it. Note that this study changes the methodology detection with respect to the
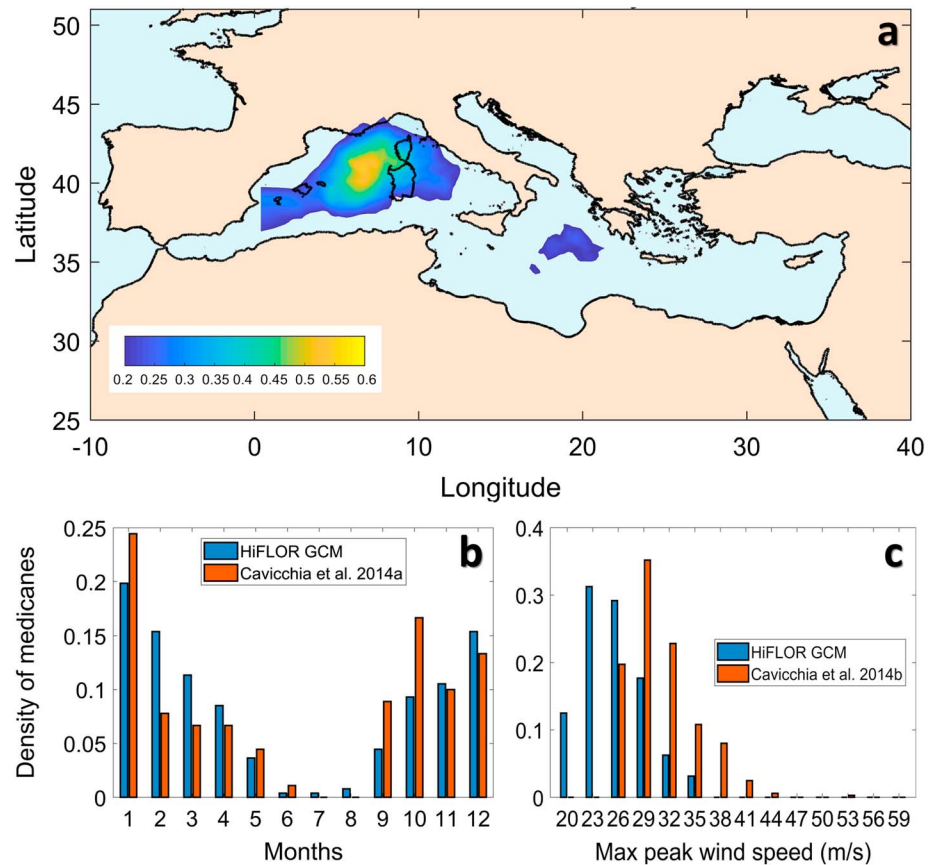
Figure 1. (a) Medicanes' track density (number per year; section 2) in CLIM, (b) monthly distribution, and (c) lifetime-maximum intensity distribution of the Medicanes in CLIM (National Centers for Environmental Prediction). HiFLOR = High-Resolution Forecast-Oriented Low Ocean Resolution; GCM = global climate model.

reference climatology (Cavicchia et al., 2014a), resulting in more Medicanes detected. Medicane's track density in Figure 1a is obtained by applying a filter (200-km radius average to avoid noisy patterns) to the number of track points per year. Number of track point is defined as the number of times when a Medicane has been in each grid point.

2.4. Power Dissipation Index

The power dissipation index (PDI [Emanuel, 2005b]) is calculated as the sum over the lifetime of the storm of the maximum surface wind speed cubed:

$$PDI = \sum_{s=1}^{\o} \sum_{\tau=1}^{d(s)} u^3(s, \tau),$$

where $\o$ is the total number of storms, d is the duration of each storm (s), and u is the wind maximum speed at each time interval (τ). Although PDI is defined herein for certain period of time, PDI can also be computed for individual storms (PDI_IS), which is equally defined but without the first summatory in s.

2.5. Tropicality Index

We define the tropicality index (TI) as the sum over the lifetime of the storm of −VTU values:

$$TI = \sum_{\tau=1}^{d(s)} -VTU(s, \tau),$$

where d is the duration of each storm (s) and $-VTU$ is thermal wind parameter for upper levels from the CPS, at each time interval (τ). In other words, TI is the accumulation of −VTU in each storm, a measure of how tropical the storm is overall.

2.6. Statistical Significance

The statistical significance analysis of the differences between periods' distributions is computed through the p value of a two-sided Wilcoxon rank sum test (Wilks, 2006). This computation tests the null hypothesis that data in x and y are samples from continuous distributions with equal medians, against the alternative that they are not. The test assumes that the two samples are independent. This test is equivalent to the Mann-Whitney U test. Unlike the Student's t test, it does not require the assumption of normal distributions and it is nearly as efficient as the Student's t test on normal distributions. Statistical significance analysis for correlations is obtained through the p value of a two-sided Student's t test. For Figure 3d, a bootstrap method is used.

2.7. Best Fit Function Calculation

The functions that best fit empirical probability distribution Figure 3a are calculated by comparing the Bayesian information criterion (Schwarz, 1978) when fitting numerous potential continuous distributions in the MATLAB software package (e.g., Beta, Exponential, Gamma, Generalized Pareto, Inverse Gaussian, Lognormal, Normal, Weibull, etc). The function with the lowest Bayesian information criterion is then selected. Generalized Pareto (Kotz & Nadarajah, 2000) distribution was found as the best fit function for each CLIM's and LATE's distributions. This distribution is often used to model the tails or extreme values of another distribution.

3. Results and Discussion

Compared to climatology (Cavicchia et al., 2014a), HiFLOR reasonably matches observational estimates of 1.9 ± 1.3 Medicanes per year in present climate conditions. Cyclones are classified as Medicanes when they acquire TC-like characteristics, that is, warm-core structure without fronts as per the Cyclone Phases Space (CPS; section 2) classification. HiFLOR reasonably reproduces the observed Medicanes' spatial distribution (Figure 1a), with a maximum south of the Gulf of Lion-Genoa (western Mediterranean), and another weaker maximum southeast of Sicily (Ionian Sea). This latter maximum is weaker probably because only a subset of Medicanes has been chosen (12 hr of warm core), compared to the reference study. The observed seasonal distribution is also well captured with a prevalence of Medicanes during the cold season months and higher frequency in winter (Figure 1b). Medicanes predominantly form from autumn to spring, when baroclinic cyclones forced by upper-level cyclonic disturbances shift southward over the Mediterranean Sea (Tous & Romero, 2013). The correlation with the observed distribution (Cavicchia et al., 2014a) is high ($r = 0.83$; p value < 0.001) and the strong observed summer minimum is reproduced too. HiFLOR tends to underestimate the wind intensity (Figure 1c), probably because of lower horizontal resolution (Cavicchia et al., 2014b; Gaertner et al., 2016).

The projected climate changes over the 21st century impact Medicane activity in the model. The frequency of Medicanes' formation is reduced by ~34% (p value < 0.01) in the LATE experiment (Figure 2a). This reduction is stronger in winter (~37%; supporting information Figure S3), and weaker in spring (~29%) and autumn (~24%). However, this lower frequency of Medicanes contrasts with their longer duration in the late 21st century RCP4.5 scenario. The number of Medicanes lasting at least 24 hr increases substantially (Figure 2b), consistently with previous studies (Gaertner et al., 2007; Tous et al., 2016). Additionally, there is a substantial shift in the Medicanes' location, with a higher density in the Ionian Sea and in proximity of South Italy's eastern coasts, and a reduction accompanied by an eastward shift in the western Mediterranean in proximity of the Balearic Islands (Figure 2c).

The reduction in Medicane frequency is likely in part due to a decrease in baroclinic precursors. Medicanes are annually correlated with ECs (section 2) with $r = 0.45$ (p value < 0.001) and ECs indeed show a decrease in number in LATE with respect to CLIM (~12%; Figure 2a), although only statistically significant at the 90% confidence level. Therefore, other factors such as a reduced mean temperature difference between the sea surface and the high troposphere (Cavicchia et al., 2014b; Romera et al., 2017) are likely to also play a role. This projected decrease in the frequency of Medicanes due to ACC is consistent with estimates (15%–60% reduction) from previous studies (Cavicchia et al., 2014b; Romera et al., 2017; Tous et al., 2016; Walsh et al., 2014). Similar conclusions about the role of ECs are reached in subtropical cyclones over the northeastern Atlantic (González-Alemán et al., 2018). The southward track shift and frequency increase of the
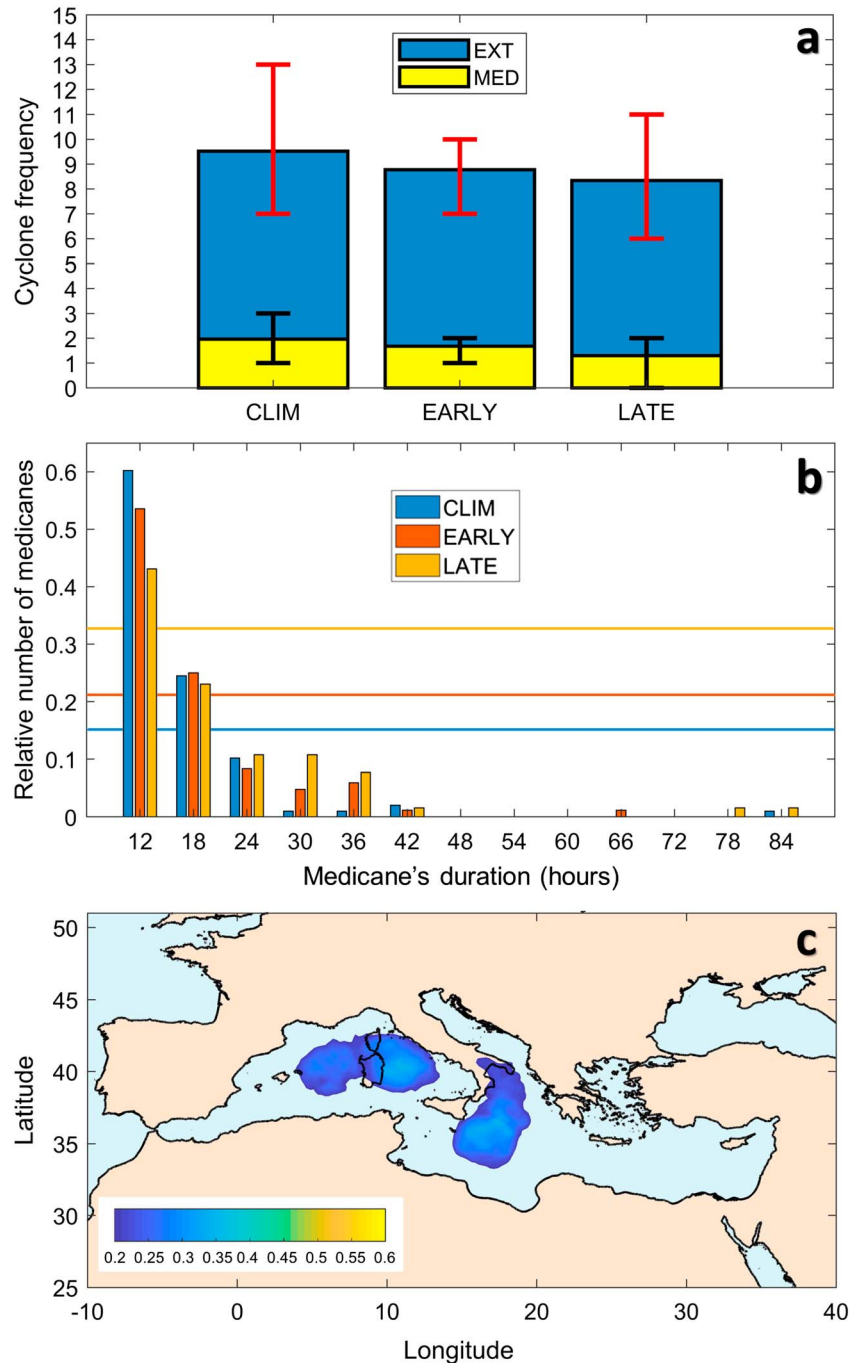
Figure 2. (a) Changes in annual Medicane (MED) and extratropical cyclone (EXT) mean frequency. Upper and lower bar indicates percentiles 75 and 25, respectively. (b) Relative number (number of Medicanes at duration divided by the total number of Medicanes in the period) of Medicanes based on their duration in hours. Also plotted (horizontal lines) is the sum of the number of Medicanes lasting at least 24 hr. (c) Medicane's track density (number per year) in LATE. CLIM = climatological run; EARLY = early future; LATE = late future.

cyclones in southern Mediterranean in the LATE run suggests that Medicanes will tend to develop more over warmer waters.

The model projects that over the 21st century Medicanes tend to be associated more frequently with stronger winds; winds exceeding 24 m s^{-1} are more recurrent in LATE run relative to CLIM (Figure 3a). We note that in these experiments, the wind speed changes in the EARLY experiment are not statistically significant
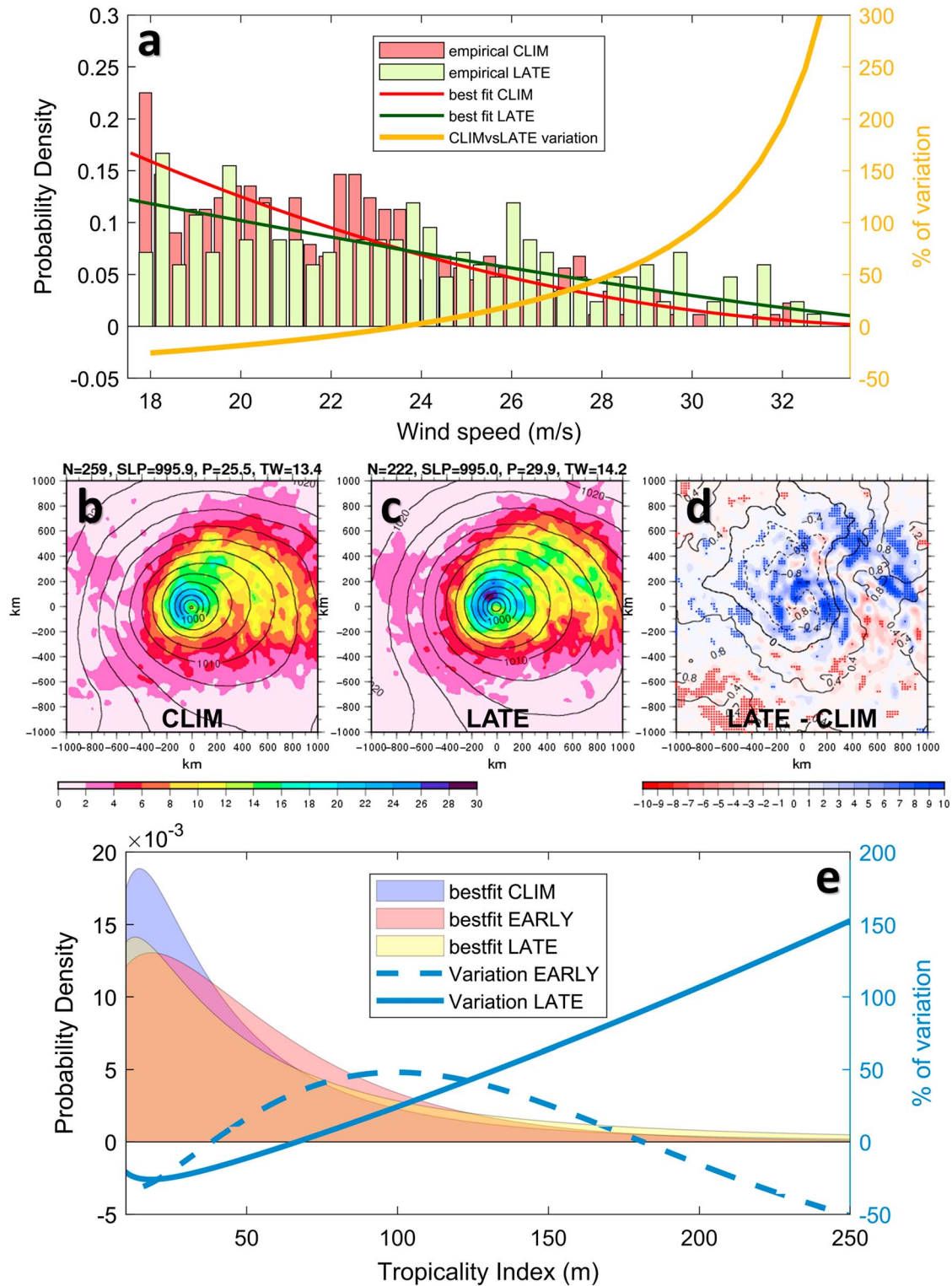
AGU
100
ADVANCING EARTH
AND SPACE SCIENCE

Geophysical Research Letters

10.1029/2018GL081253

Figure 3. (a) Probability distribution for 10-m wind speed associated with the medicane stages. Also plotted are the probability density functions that best fit (section 2) each empirical probability distribution. Orange function is the percentage of variation of LATE's function with respect to CLIM's function. (b) Composites of accumulated precipitation (shaded; mm/day) and sea level pressure (black contours) for Medicanes in their tropical stages in CLIM. N is the number of the sample, SLP is the minimum sea level pressure, P is the maximum precipitation, and TW is the maximum tangential wind speed. (c) Same as (b) but for LATE. (d) Same as (b) and (c) but for differences between LATE and CLIM. Statistical significant differences (at the 90% confidence level) are highlighted by strong color. (e) Probability density functions that best fit (section 2) each empirical probability distribution for tropicality index. Blue function is the percentage of variation with respect to CLIM. CLIM = climatological run; EARLY = early future; LATE = late future.
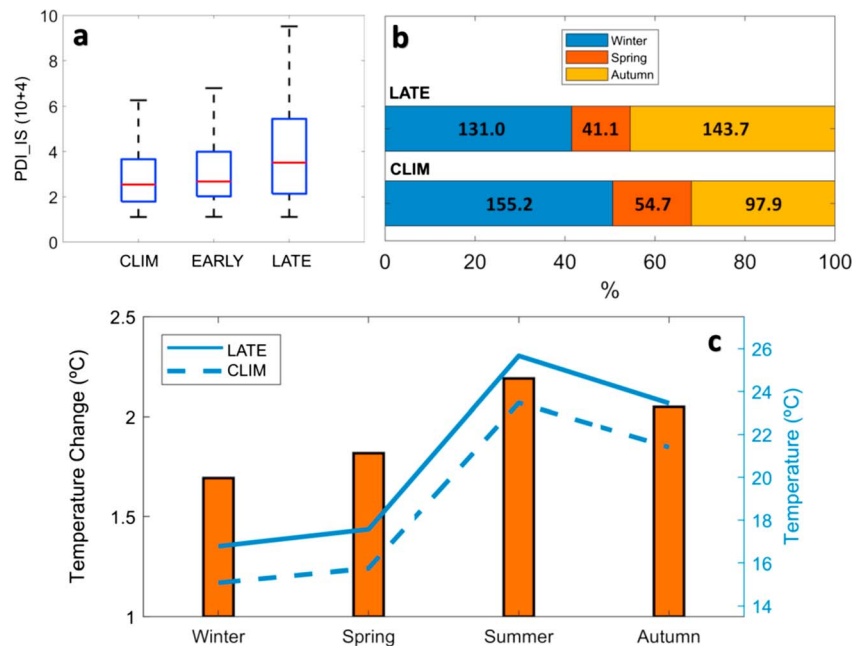
Figure 4. (a) Boxplot for PDI_IS's distribution. (b) Percentage of power dissipation index (PDI) contribution of each season to the annual PDI in each 50-year run. Real PDI values (10^{+04} m^3/s^2) are indicated within each bar. (c) Sea surface temperatures value and change (LATE vs. CLIM) for each season. CLIM = climatological run; EARLY = early future; LATE = late future; PDI = power dissipation index.

(supporting information Figure S4). The strongest tangential winds typically occur from the maximum wind radius (~100 km) outward (supporting information Figure S5a). This radius is higher than in most observed cases (e.g., Cavicchia et al., 2014a) and is probably related to the grid spacing used herein (Pielke, 1991). The projected increase in Medicane winds is most evident in autumn (supporting information Figure S6). Precipitation associated with Medicanes is also a serious hazard as they can cause coastal flash floods (Reale & Atlas, 2001). In Figure 3, we compute composites of rainfall in CLIM and LATE. Precipitation significantly increases (Figure 3d) in the LATE run relative to the CLIM run, especially in the inner zone (100–300 km from the center, supporting information Figure S5b). This confirms that they become more hazardous regarding rainfall impact.

Is the projected future increase in Medicane wind intensity associated with Medicanes developing a more robust tropical structure and thus stronger and deeper convection in the core? This effect can be measured by the thermal wind parameter for the upper tropospheric layer (−VTU; section 2), which describes the upper thermal anomaly in the 3-D structure of the cyclone, with values above 0 indicating a warm core. We find that in Medicanes −VTU values are correlated ($r = 0.34$; p value < 0.001) with the surface wind speed, in CLIM + EARLY + LATE. This indicates that the more robust their tropical structure, the stronger the near-surface winds. −VTU's median in LATE, as opposed to EARLY, is statistically different from −VTU's median in CLIM, with a noticeable increase in the upper percentiles, as for the wind. This suggests that Medicanes in the future will be more likely to achieve higher intensity because of a more robust tropical structure within their central region. This implies stronger convection and thus a larger release of latent heating, which in turns leads to a higher radial pressure gradient, thus increasing wind speed (Figure 3a, and supporting information Figure S5a). Changes in convective activity have been linked to wind intensity in the case of TCs (Jiang, 2012). Indeed, the relationship between wind and -VTU is much higher in LATE ($r = 0.45$; p value < 0.001) than in CLIM ($r = 0.28$; p value < 0.001). This indicates that wind speed is more sensitive to the depth of the upper-level warm core (moist convection activity) in ACC context, and could even point to wind-induced surface heat exchange (Emanuel, 1986) feedback being more effective. This concept is better highlighted by the change in the Tropicality Index (TI; section 2), an overall measure quantifying the degree to which a Medicane is tropical in structure (or maturity). Figure 3e shows higher values of TI

noticeably increasing in LATE, as opposed to EARLY run, where the increase only occurs at moderate values.

The concurrent increase in Medicanes' intensity and duration are suggestive of an increase in their hazard to natural and human resources. To better quantify this, we analyze the PDI (PDI_IS; section 2). PDI_IS quantifies the power dissipated by the near-surface winds acting on the surface, thus being a measure of the destructiveness of Medicanes. We find a remarkable positive statistical change in PDI_IS in the late 21st century run as compared to the 1986–2005 and 2016–2035 runs (Figure 4a), which confirms their higher destructive effects in the late future. For the PDI (a measure for the overall activity; section 2), an increase is also found for the LATE experiment compared to CLIM (from ~$308 \cdot 10^{+04}$ to ~$316 \cdot 10^{+04}$ m^3/s^2; Figure 4 b), which is consistent with the idea of each Medicane being more durable and intense, since they are less frequent in LATE. This increase is exclusively due to the notable positive change (~47%) during autumn (Figure 4b), whereas the PDI decreases in the rest of the seasons (summer has marginal contribution). This notable contribution from the autumn season is consistent with the more hurricane-like structure of Medicanes, and it could be related to the enhanced autumn SSTs warming relative to spring and winter (Figure 4c). This relationship between PDI and SSTs has been explained through the SSTs positive influences on the potential intensity of TCs, which is related to alterations of the surface energy flux (Emanuel, 1987). However, no robust evidence is obtained when analyzing PDI changes in the future for TCs (Knutson et al., 2013).

4. Conclusions

In conclusion, by using a global high-resolution coupled GCM under an intermediate-emission 21st century scenario (RCP4.5), we found a number of dramatic shifts in Medicane-related hazards by the end of the 21st century. Although our results are based on a single model, this is the first global coupled model capable to reproduce the basic physics of Medicanes and featuring a horizontal grid spacing (~25 km) high enough to reproduce their mesoscale circulation. While fewer in number, Medicanes are likely to become more vigorous in autumn relative to spring and winter and to develop long-lasting deeper warm cores, that is, more robust tropical structure, increasing the likelihood of achieving hurricane intensity. This more tropical nature of Medicanes is also accompanied by projections of more intense precipitation—mirroring projections of precipitation change by U.S. landfalling hurricanes (Liu et al., 2018). More intense precipitation is also a cause for concern given flood risks posed by these storms. Additionally, Medicanes tend to change their favored genesis and passage location, becoming more common in the Ionian Sea and less common in the western Mediterranean Sea. However, it is important to note some limitations arising from both the resolution of the ocean and atmospheric components of the model, which could still be insufficient to realistically simulate specific mesoscale characteristics of Medicanes and the Mediterranean Sea. Significant changes in the Medicanes' activity is found only in late future conditions as opposed to early future, indicating that Medicanes are not likely going to change substantially in the next few decades but will be significantly affected by ACC by the end of the 21st century. In the RCP4.5 scenario assumed here, considerable efforts are required to reduce the cumulative emissions of greenhouse gases. Stronger-emission scenarios like the RCP8.5 (van Vuuren et al., 2011) would see an even stronger global temperature change by the end of the 21st century (~5–9 °C) and a warmer Mediterranean Sea, thus amplifying even more the Medicanes' potential destructiveness in response to ACC. These changes found in Medicane activity potentially increase their societal and natural damage, and the shifting locations of these risks will affect populations previously unaccustomed, thus enhancing the potential damage.

References

Akhtar, N., Brauch, J., Dobler, A., Béranger, K., & Ahrens, B. (2014). Medicanes in an ocean-atmosphere coupled regional climate model. *Natural Hazards and Earth System Sciences*, 14, 2189–2201. https://doi.org/10.5194/nhess-14-2189-2014

Bhatia, K., Vecchi, G., Murakami, H., Underwood, S., & Kossin, J. (2018). Projected response of tropical cyclone intensity and intensification in a global climate model. *Journal of Climate*, 31, 8281–8303. https://doi.org/10.1175/JCLI-D-17-0898.1

Cavicchia, L., von Storch, H., & Gualdi, S. (2014a). A long-term climatology of medicanes. *Climate Dynamics*, 43, 1183–1195. https://doi.org/10.1007/s00382-013-1893-7

Cavicchia, L., Von Storch, H., & Gualdi, S. (2014b). Mediterranean tropical-like cyclones in present and future climate. *Journal of Climate*, 27, 7493–7501. https://doi.org/10.1175/JCLI-D-14-00339.1

Collins, M., Knutti, R., Arblaster, J., Dufresne, J.-L., Fichefet, T., Friedlingstein, P., et al. (2013). Chapter 12 - Long-term climate change: Projections, commitments and irreversibility. In *Climate Change 2013: The Physical Science Basis. IPCC Working Group I Contribution to AR5. Eds. IPCC*. Cambridge: Cambridge University Press.

Delworth, T. L., Rosati, A., Anderson, W. G., Adcroft, A. J., Balaji, V., Benson, R., et al. (2012). Simulated climate and climate change in the GFDL CM2.5 high-resolution coupled climate model. *Journal of Climate*, 25, 2755–2781. https://doi.org/10.1175/JCLI-D-11-00316.1

Delworth, T. L., & Zeng, F. (2014). Regional rainfall decline in Australia attributed to anthropogenic greenhouse gases and ozone levels. *Nature Geoscience*, 7, 583–587. https://doi.org/10.1038/ngeo2201

Delworth, T. L., Zeng, F., Vecchi, G. A., Yang, X., Zhang, L., & Zhang, R. (2016). The North Atlantic Oscillation as a driver of rapid climate change in the Northern Hemisphere. *Nature Geoscience*, 9, 509–512. https://doi.org/10.1038/ngeo2738

Emanuel, K. (2005a). Genesis and maintenance of "Mediterranean hurricanes". *Advances in Geosciences*, 2(1987), 217–220. https://doi.org/10.5194/adgeo-2-217-2005

Emanuel, K. (2005b). Increasing destructiveness of tropical cyclones over the past 30 years. *Nature*, 436(7051), 686–688. https://doi.org/10.1038/nature03906

Emanuel, K. A. (1986). An air-sea interaction theory for tropical cyclones. Part I: Steady-state maintenance. *Journal of the Atmospheric Sciences*, 43(6), 585–605. https://doi.org/10.1175/1520-0469(1986)043<0585:AASITF>2.0.CO;2

Emanuel, K. A. (1987). The dependence of hurricane intensity on climate. *Nature*, 326(6112), 483–485. https://doi.org/10.1038/326483a0

Gaertner, M. Á., González-Alemán, J. J., Romera, R., Domínguez, M., Gil, V., Sánchez, E., et al. (2016). Simulation of medicanes over the Mediterranean Sea in a regional climate model ensemble: Impact of ocean–atmosphere coupling and increased resolution. *Climate Dynamics*, 1–17. https://doi.org/10.1007/s00382-016-3456-1

Gaertner, M. a., Jacob, D., Gil, V., Domínguez, M., Padorno, E., Sánchez, E., & Castro, M. (2007). Tropical cyclones over the Mediterranean Sea in climate change simulations. *Geophysical Research Letters*, 34, L14711. https://doi.org/10.1029/2007GL029977

González-Alemán, J. J., Gaertner, M. A., Sánchez, E., & Romera, R. (2018). Subtropical cyclones near-term projections from an ensemble of regional climate models over the northeastern Atlantic basin. *International Journal of Climatology*, 38, e454–e465. https://doi.org/10.1002/joc.5383

Hart, R. E. (2003). A cyclone phase space derived from thermal wind and thermal asymmetry. *Monthly Weather Review*, 131(4), 585–616. https://doi.org/10.1175/1520-0493(2003)131<0585:ACPSDF>2.0.CO;2

Jiang, H. (2012). The relationship between tropical cyclone intensity change and the strength of inner-core convection. *Monthly Weather Review*, 140, 1164–1176. https://doi.org/10.1175/MWR-D-11-00134.1

Kapnick, S. B., Delworth, T. L., Ashfaq, M., Malyshev, S., & Milly, P. C. D. (2014). Snowfall less sensitive to warming in Karakoram than in Himalayas due to a unique seasonal cycle. *Nature Geoscience*, 7, 834–840. https://doi.org/10.1038/ngeo2269

Knutson, T. R., Sirutis, J. J., Vecchi, G. A., Garner, S., Zhao, M., Kim, H. S., et al. (2013). Dynamical downscaling projections of twenty-first-century Atlantic hurricane activity: CMIP3 and CMIP5 model-based scenarios. *Journal of Climate*, 26(17), 6591–6617. https://doi.org/10.1175/JCLI-D-12-00539.1

Køltzow, M. A. Ø., Iversen, T., & Haugen, J. E. (2011). The importance of lateral boundaries, surface forcing and choice of domain size for dynamical downscaling of global climate simulations. *Atmosphere*, 2(2), 67–95. https://doi.org/10.3390/atmos2020067

Kotz, S., & Nadarajah, S. (2000). Extreme value distributions. Theory and Applications. doi:https://doi.org/10.1007/978-3-642-04898-2

Li, G., & Xie, S. P. (2012). Origins of tropical-wide SST biases in CMIP multi-model ensembles. *Geophysical Research Letters*, 39, L22703. https://doi.org/10.1029/2012GL053777

Liu, M., Vecchi, G. A., Smith, J. A., & Murakami, H. (2018). Projection of Landfalling-tropical cyclone rainfall in the Eastern United States under anthropogenic warming. *Journal of Climate*, 31, 7269–7286. https://doi.org/10.1175/JCLI-D-17-0747.1

Lorenz, P., & Jacob, D. (2005). Influence of regional scale information on the global circulation: A two-way nesting climate simulation. *Geophysical Research Letters*, 32, L18706. https://doi.org/10.1029/2005GL023351

Moscatello, A., Miglietta, M. M., & Rotunno, R. (2008). Numerical analysis of a Mediterranean "hurricane" over southeastern Italy. *Monthly Weather Review*, 136(11), 4373–4397. https://doi.org/10.1175/2008MWR2512.1

Murakami, H., Levin, E., Delworth, T. L., Gudgel, R., & Hsu, P.-C. (2018). Dominant effect of relative tropical Atlantic warming on major hurricane occurrence. *Science*. Retrieved from http://science.sciencemag.org/content/early/2018/09/26/science.aat6711.abstract, 362(6416), 794–799. https://doi.org/10.1126/science.aat6711

Murakami, H., Vecchi, G. A., & Underwood, S. (2017). Increasing frequency of extremely severe cyclonic storms over the Arabian Sea. *Nature Climate Change*, 7(12), 885–889. https://doi.org/10.1038/s41558-017-0008-6

Murakami, H., Vecchi, G. A., Underwood, S., Delworth, T. L., Wittenberg, A. T., Anderson, W. G., et al. (2015). Simulation and prediction of category 4 and 5 hurricanes in the high-resolution GFDL HiFLOR coupled climate model. *Journal of Climate*, 28(23), 9058–9079. https://doi.org/10.1175/JCLI-D-15-0216.1

Murakami, H., Vecchi, G. A., Villarini, G., Delworth, T. L., Gudgel, R., Underwood, S., et al. (2016). Seasonal forecasts of major hurricanes and landfalling tropical cyclones using a high-resolution GFDL coupled climate model. *Journal of Climate*, 29(22), 7977–7989. https://doi.org/10.1175/JCLI-D-16-0233.1

Pascale, S., Boos, W. R., Bordoni, S., Delworth, T. L., Kapnick, S. B., Murakami, H., et al. (2017). Weakening of the North American monsoon with global warming. *Nature Climate Change*, 7(11), 806–812. https://doi.org/10.1038/nclimate3412

Picornell, M. A., Jansà, A., Genovés, A., & Campins, J. (2001). Automated database of mesocyclones from the HIRLAM (INM)-0.5° analyses in the western Mediterranean. *International Journal of Climatology*, 21(3), 335–354. https://doi.org/10.1002/joc.621

Pielke, R. A. (1991). A recommended specific definition of "resolution". *Bulletin of the American Meteorological Society*, 72(12), 1914–1914.

Reale, O., & Atlas, R. (2001). Tropical cyclone-like vortices in the extratropics: Observational evidence and synoptic analysis. *Weather and Forecasting*, 16(1), 7–34. https://doi.org/10.1175/1520-0434(2001)016<0007:TCLVIT>2.0.CO;2

Ricchi, A., Miglietta, M. M., Barbariol, F., Benetazzo, A., Bergamasco, A., Bonaldo, D., et al. (2017). Sensitivity of a Mediterranean tropical-like cyclone to different model configurations and coupling strategies. *Atmosphere*, 8(12). https://doi.org/10.3390/atmos8050092

Romera, R., Gaertner, M. Á., Sánchez, E., Domínguez, M., González-Alemán, J. J., & Miglietta, M. M. (2017). Climate change projections of medicanes with a large multi-model ensemble of regional climate models. *Global and Planetary Change*, 151, 134–143. https://doi.org/10.1016/j.gloplacha.2016.10.008

Schade, L. R., & Emanuel, K. a. (1999). The ocean's effect on the intensity of tropical cyclones: Results from a Simple Coupled Atmosphere–Ocean Model. *Journal of the Atmospheric Sciences*, 56(4), 642–651. https://doi.org/10.1175/1520-0469(1999)056<0642:TOSEOT>2.0.CO;2

Schwarz, G. E. (1978). Estimating the dimension of a model. *Annals of Statistics*, 6(2), 461–464. https://doi.org/10.1214/aos/1176344136, MR 0468014

Tous, M., & Romero, R. (2013). Meteorological environments associated with medicane development. *International Journal of Climatology*, *33*(1), 1–14. https://doi.org/10.1002/joc.3428

Tous, M., Zappa, G., Romero, R., Shaffrey, L., & Vidale, P. L. (2016). Projected changes in medicanes in the HadGEM3 N512 high-resolution global climate model. *Climate Dynamics*, *47*(5–6), 1913–1924. https://doi.org/10.1007/s00382-015-2941-2

van der Wiel, K., Kapnick, S. B., & Vecchi, G. A. (2017). Shifting patterns of mild weather in response to projected radiative forcing. *Climatic Change*, *140*, 649–658. https://doi.org/10.1007/s10584-016-1885-9

van Vuuren, D. P., Edmonds, J., Kainuma, M., Riahi, K., Thomson, A., Hibbard, K., et al. (2011). The representative concentration pathways: An overview. *Climatic Change*, *109*(1-2), 5–31. https://doi.org/10.1007/s10584-011-0148-z

Vecchi, G. A., Delworth, T., Gudgel, R., Kapnick, S., Rosati, A., Wittenberg, A. T., et al. (2014). On the seasonal forecasting of regional tropical cyclone activity. *Journal of Climate*, *27*(21), 7994–8016. https://doi.org/10.1175/JCLI-D-14-00158.1

Walsh, K., Giorgi, F., & Coppola, E. (2014). Mediterranean warm-core cyclones in a warmer world. *Climate Dynamics*, *42*(3–4), 1053–1066. https://doi.org/10.1007/s00382-013-1723-y

Wilks, D. S. (Department of E., & University), A. S. C(2006). Statistical methods in the atmospheric sciences. *Meteorological Applications*, *14*.

Zhang, W., Vecchi, G. A., Murakami, H., Delworth, T., Wittenberg, A. T., Rosati, A., et al. (2016). Improved simulation of tropical cyclone responses to ENSO in the western North Pacific in the high-resolution GFDL HiFLOR coupled climate model. *Journal of Climate*, *29*(4), 1391–1415. https://doi.org/10.1175/JCLI-D-15-0475.1